Journal of Power Sources 184 (2008) 9–15

Contents lists available at ScienceDirect

Journal of Power Sources

journal homepage: www.elsevier.com/locate/jpowsour

Performance evaluation of passive direct methanol fuel cell with methanol vapour supplied through a flow channel

Ikwhang Chang[a], Seungbum Ha[b], Jinho Kim[c], JaeYong Lee[c], Suk Won Cha[b,*]

[a] Interdisciplinary Program in Automotive Engineering, Seoul National University, San 56-1, Sillim9-dong, Kwanak-gu, Seoul 151-744, Republic of Korea
[b] Department of Mechanical and Aerospace Engineering, Seoul National University, San 56-1, Sillim9-dong, Kwanak-gu, Seoul 151-744, Republic of Korea
[c] Samsung Advanced Institute of Technology, San 14-1, Nongseo-Dong, Giheung-Gu, Yongin-Si, Gyeonggi-do 449-712, Republic of Korea

ARTICLE INFO

Article history:
Received 13 April 2008
Received in revised form 20 May 2008
Accepted 2 June 2008
Available online 21 June 2008

Keywords:
Direct methanol fuel cell
Passive
Vapour feed
Air-breathing
Flow channel
Humidified membrane electrode assembly

ABSTRACT

This work examines the effect of fuel delivery configuration on the performance of a passive air-breathing direct methanol fuel cell (DMFC). The performance of a single cell is evaluated while the methanol vapour is supplied through a flow channel from a methanol reservoir connected to the anode. The oxygen is supplied from the ambient air to the cathode via natural convection. The fuel cell employs parallel channel configurations or open chamber configurations for methanol vapour feeding. The opening ratio of the flow channel and the flow channel configuration is changed. The opening ratio is defined as that between the area of the inlet port and the area of the outlet port. The chamber configuration is preferred for optimum fuel feeding. The best performance of the fuel cell is obtained when the opening ratio is 0.8 in the chamber configuration. Under these conditions, the peak power is 10.2 mW cm^{-2} at room temperature and ambient pressure. Consequently, passive DMFCs using methanol vapour require sufficient methanol vapour feeding through the flow channel at the anode for best performance. The mediocre performance of a passive DMFC with a channel configuration is attributed to the low differential pressure and insufficient supply of methanol vapour.

1. Introduction

The direct methanol fuel cell (DMFC) is one of the most promising portable power sources for mobile electronic devices (e.g., laptops, cellular phones, and PDAs). The advantages of DMFCs are reasonably high specific energy, convenient storage of fuel, and low temperature operation [1,2]. Nevertheless, DMFCs have several problems and technological issues that still need to be addressed to improve their performances for example: methanol crossover, high catalyst loading and low power density [3–5]. In a DMFC, a fraction of methanol fuel at the anode is transported to the cathode under the influence of a concentration gradient. This is called 'methanol crossover'. The transported methanol reacts directly with the oxygen at the cathode. In this situation, no current is produced even though the fuel cell consumes the methanol fuel. The rate of methanol crossover is strongly proportional to the methanol concentration at the anode [6]. Additionally, methanol, which is toxic, lowers the activity of the catalyst and degrades the cell performance [7]. In DMFCs, the methanol fuel is delivered to the anode either actively or passively. The same applies to the delivery of air to the cathode. Active feeding requires auxiliary devices, such as pumps or blowers, to deliver the fuel and oxygen to the gas-diffusion layer of the respective electrode. Conversely, passive systems do not need any power to supply fuel and oxygen. Therefore, passive DMFCs can minimize the auxiliary system volume, parasitic losses and system control. Although passive DMFCs are preferred for mobile power sources because of these advantages, their power outputs do not satisfy the power demands of various electrical devices. To improve the performance of passive DMFCs, the following factors must be considered: methanol concentration, membrane properties such as thickness, the structure of membrane electrode assembly (MEA), and overall details of the system configuration [8].

Bae et al. [9] reported the evaluation of passive DMFCs fed with liquid methanol. The optimum methanol concentration was 5 M at the anode, and the catalyst loading of each electrode was 8 mg cm^{-2}. Kim [10] proposed a MEA that passively fed water to the anode by itself. It utilized pure methanol as fuel and could produce around 20–30 mW cm^{-2} for 15 days. The system adopted a porous buffer to control the water supply at the anode passively. For characterization of the passive DMFC, the power was measured under a fixed voltage of 0.3–0.35 V (potentiostat mode), at which the cell generated maximum power [10]. Typically, the power output of a DMFC fluctuates widely during long-term operation. In a passive DMFC, the required water at the anode is supplied from the cathode by back-diffusion. Therefore, the supply of water is unstable. This instability lowers the performance of a passive DMFC. To

* Corresponding author. Tel.: +82 2 880 8050; fax: +82 2 883 1513.
E-mail address: swcha@snu.ac.kr (S.W. Cha).

0378-7753/$ – see front matter.
doi:10.1016/j.jpowsour.2008.06.036

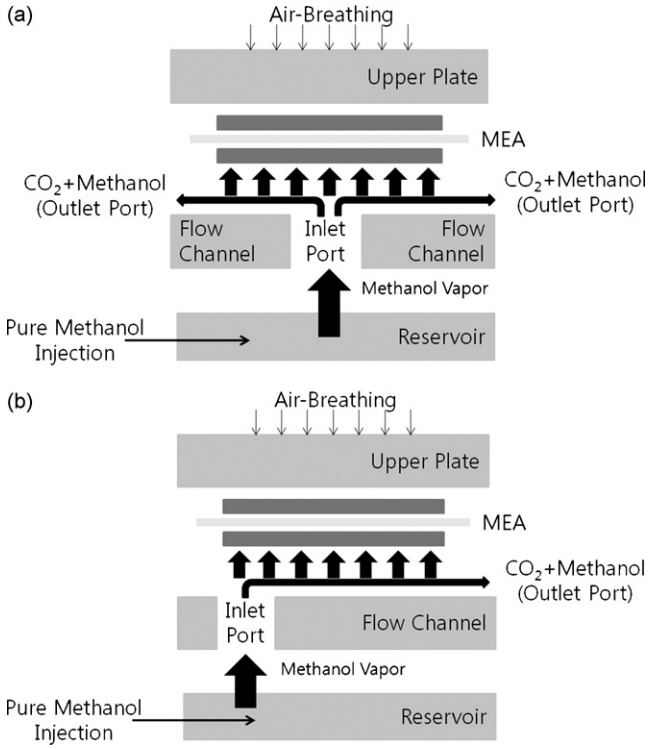

Fig. 1. Schematic of passive DMFC fuelled by methanol vapour from reservoir to MEA: (a) central inlet and (b) side inlet.

obtain maximum power, in spite of MEA degradation, low-voltage operation could be preferred [11–13].

One approach to improve the performance of a passive DMFC is to use methanol vapour as fuel. Schematic diagrams of examples of such passive DMFCs are shown in Fig. 1. The methanol is temporarily stored in a reservoir adjacent to the flow channel. After the methanol vapourizes in the reservoir, the vapour progresses through the flow channel and then the gas-diffusion layer of the anode. After the electrochemical reaction, carbon dioxide and any remaining methanol vapour exit from the system.

The work presented here examines the effect of various flow channel configurations on a performance of a DMFC using pure methanol vapour as the fuel at the anode. In particular, to improve the power density, the optimum opening ratio between the inlet and outlet ports of the flow channel has been investigated. The performance of a single cell at room temperature and ambient pressure has been evaluated as a passive air-breathing system. This experiment follows the typical requirements of portable fuel cells for mobile application [14–16].

2. Fuel cell design and experimental set-up

The design of the fuel-cell assembly comprises the following components: methanol reservoir, flow channel (Figs. 2–4), gasket, MEA, and upper plate for air-breathing (Fig. 5). The overall dimensions of the assembly are 60 mm (W) × 60 mm (B) × 20 mm (H). The following sections describe each component in detail.

2.1. Methanol reservoir

To obtain both strength and simplicity of manufacturing, polycarbonate has been chosen for the frame material. The key factor in making this selection is rigidity to maintain the tightness of sealing between the MEA and the frame. The total area of the

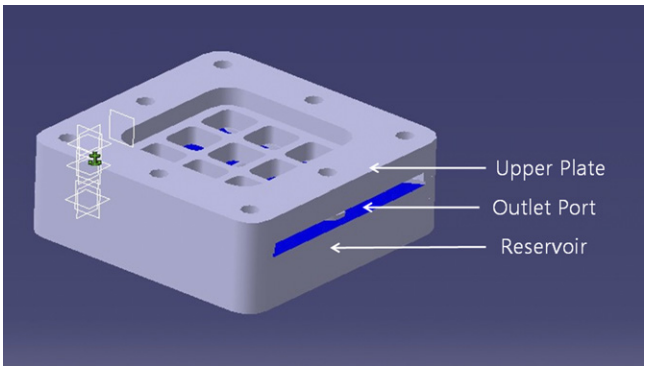

Fig. 2. Schematic assembly of single cell.

methanol reservoir is 2.45 cm^2. A port of 1.5 mm diameter is drilled for methanol delivery to the reservoir. Pure methanol from a syringe pump is supplied to the reservoir through a port at a fixed rate of 0.4 ml h^{-1}. Inside the reservoir, the methanol is absorbed in foam temporarily, before it evaporates.

2.2. Flow channel

In designing the flow channels, the following factors have been investigated: the ratio between the inlet and outlet ports of the

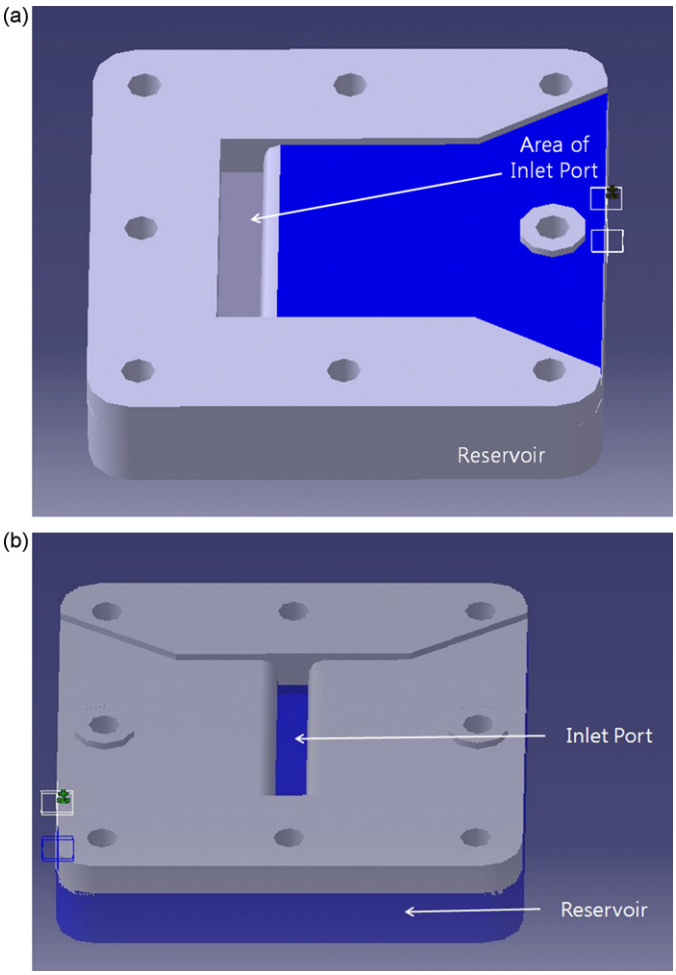

Fig. 3. Position details of inlet and outlet in chamber configuration: (a) side inlet and (b) central inlet.

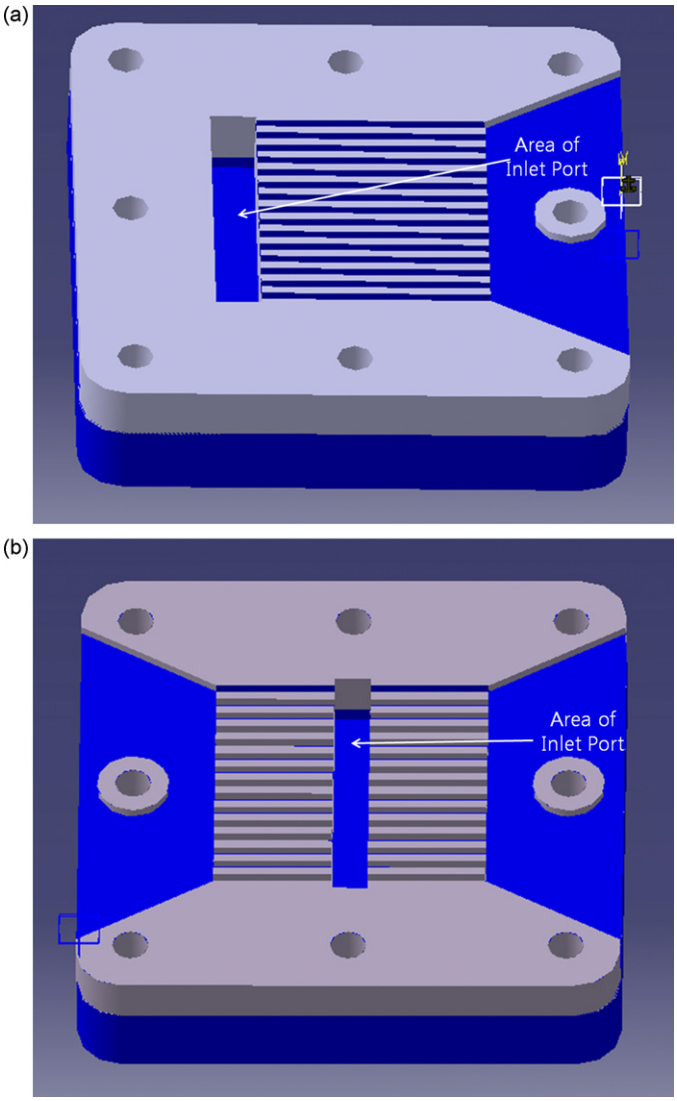

Fig. 4. Position details of inlet and outlet in parallel-channel configuration: (a) side inlet and (b) central inlet.

anode channel, the actual shape of the channel, and the area of the air-breathing element at the cathode. Various flow channel shapes and opening ratios at the anode have been investigated. Serpentine channel design, however, was dismissed due to insufficient fuel delivery resulting from excessive pressure drop along the flow channel. The position of the inlet was specifically divided into two types, namely, central and side inlet types, and the area of each was 1.2 and 1.5 cm^2, respectively. Also, the area of the outlet was 0.47 cm^2 for both cases. The height and depth of the flow channel is 1 mm, and two widths of the flow channel are employed; namely: parallel channel 2 mm and parallel channel 1 mm. The specifications of each flow channel are listed in Table 1, such as flow channel length, opening ratio, channel/rib width, and position of inlet. Among these parameters, the opening ratio is defined as follows (Figs. 6 and 7):

$$\text{Opening ratio} = \frac{\text{area of outlet port}}{\text{area of inlet port}} \quad (1)$$

The flow channel, which has an exit for carbon dioxide, is quite different from other passive DMFCs, because almost all passive fuel feeding DMFC systems do not have an exit for the carbon dioxide

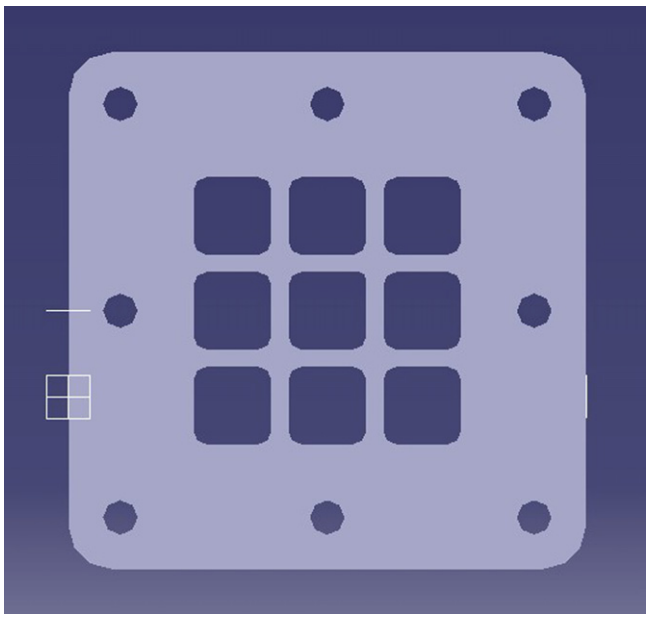

Fig. 5. Upper plate design for air-breathing in cathode.

Table 1
Specifications of flow channels

Channel type	Channel length (mm)	Channel/rib width (mm)	Opening ratio	Position of inlet
Parallel	26	1	0.8	Central inlet
Parallel	25	1	0.5	Side inlet
Parallel	25	1	0.3	Side inlet
Parallel	26	2	0.8	Central inlet
Parallel	25	2	0.3	Side inlet
Chamber	26	–	0.8	Central inlet
Chamber	25	–	0.5	Side inlet
Chamber	25	–	0.3	Side inlet

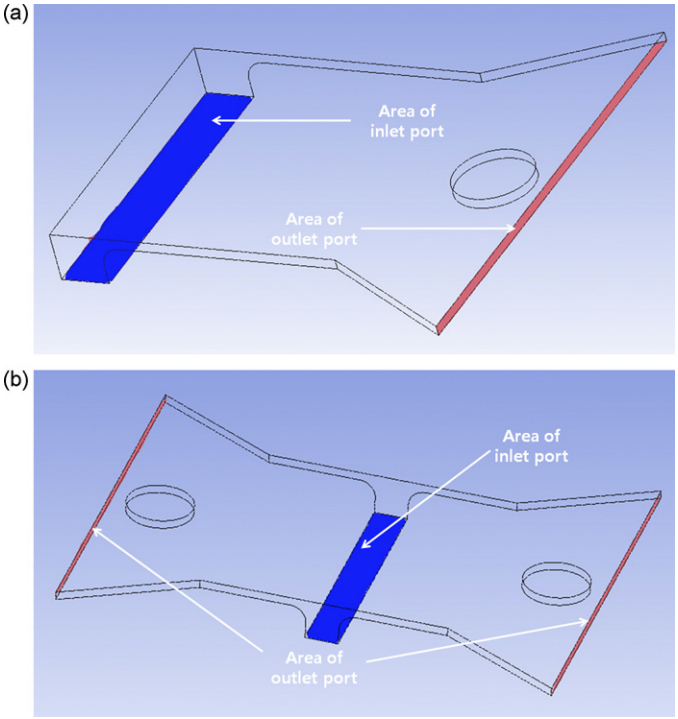

Fig. 6. Schematic design of opening ratio in chamber configuration: (a) side inlet and (b) central inlet.

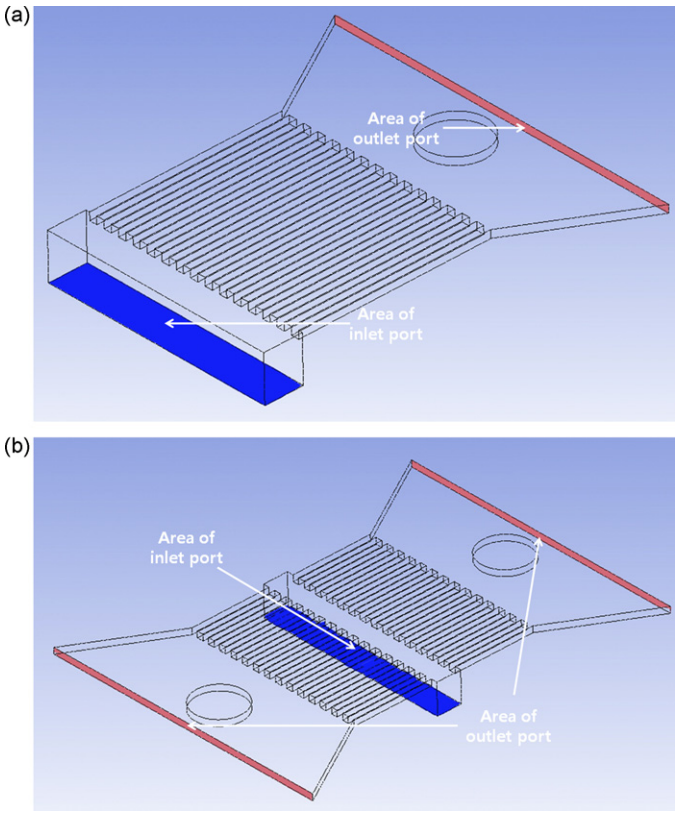

Fig. 7. Schematic design of opening ratio in parallel-channel configuration: (a) side inlet and (b) central inlet.

at the anode, namely, they are closed systems [9,10,17]. Therefore, the effect of the carbon dioxide exit on cell performance may not have been estimated in other designs.

2.3. Upper plate

The important role of the upper plate is to expose the cathode to the ambient environment for the air-breathing element. It has been reported [18] that optimum opening ratio at the cathode for a passive fuel cell is around 71% and the opening shape is square. In the present design, an opening ratio of 69% is employed. The dimensions of air-breathing at the cathode are 36 mm (W) × 36 mm (B). The air-breathing holes have a square shape, and the dimension of square hole is 10 mm (W) × 10 mm (B). The gap between the square holes is 2 mm (Fig. 5).

2.4. Gasket

In order to prevent leakage of fuel and oxidation of the catalyst by ambient air, good sealing of the MEA is critical problem in passive DMFCs [19]. In particular, since the compressibility of gasket material and compression force inside the cell strongly affect the contact resistance and the gas diffusivity of MEA, selecting a good gasket material is important. A high compression force prevents proper fuel supply through the gas-diffusion layer. Conversely, a low compression force increases the contact resistance between the current-collector and the electrode. Teflon sheet of 230 μm was selected as the gasket material, and the optimum compression was obtained by controlling the tightening torque of the assembly bolts at 120 N cm^{-2}.

2.5. Membrane electrode assembly

The dimensions of the MEA was 9 cm^2 (3 cm × 3 cm). The electrolyte membrane was fabricated by a solution-casting method and had a thickness of 50 μm [10]. PtRu black and Pt black were used as the catalyst for the anode and cathode, respectively. The catalyst loadings for the anode and cathode were 8 mg cm^{-2} for both. The anode diffusion layer was made of a carbon-backing layer with silica particles of 4–5 nm and polyvilyldiene fluoride (PVDF). For the cathode diffusion layer, a mixture of carbon particles and polytetrafluoro ethylene (PTFE) was first sprayed on to the carbon-backing layer with a loading of 2 mg cm^{-2}. SGL plain paper and Toray 090 carbon paper were used for the anode-backing layer and the cathode-backing layer, respectively. Gold-coated nickel-mesh integrated with the MEA served as a current-collector [10,20].

2.6. Experiment setup

Before the main experiments, the cell went through an activation process at room temperature. The open-circuit voltage (OCV) was measured over 30 min, and the cell was operated for about 24 h at 0.35 V. Polarization curves were obtained by mean of a Solartron 1287 potentiostat. The liquid methanol was supplied to the reservoir by a syringe pump at 0.4 ml h^{-1} continuously and the methanol in the reservoir evaporated into the flow channels. The water required at the anode was back-diffused from the cathode. The temperature was measured on the cathode surface using thermocouples in only long-term operation to identify the relationship between performance fluctuations and temperature variations. For polarization curves, the temperature was not measured due to the intended purpose for mobile application, and ambient pressure as well as room temperature were the conditions for the air-breathing passive DMFC.

3. Experimental results and discussions

3.1. Influence of flow channel

Fig. 8 gives a comparison of the open-circuit voltage obtained from different flow channel configurations, i.e., parallel channel (2 mm), parallel channel (1 mm), and chamber. The parallel channel (1 mm) and the parallel channel (2 mm) have the same opening ratio of 0.3. The opening ratio of chamber is 0.8. The OCV was stabilized around 0.46 V, regardless of the flow channel types, in 30 min. Fig. 9 shows how different flow channel configurations affect the cell performance. The chamber configuration achieved the highest power density of 8.5 mW cm^{-2}. Conversely, the power density of the parallel channel (1 mm) and the parallel channel (2 mm) are less than 5.4 mW cm^{-2}. The low performance of the parallel channel configurations can be attributed to insufficient methanol supply in the flow channel that diffuses to the anode catalyst layer. Compared with forced methanol feeding in an active cell, methanol vapour is transported more slowly from the flow channel to the gas-diffusion layer, and the low differential pressure does not force methanol vapour to travel to the catalyst layer. Also, since the dividing rib in parallel channels blocks methanol diffusion for the electrochemical reactions, the transport of methanol vapour in the chamber configuration is more effective in passive DMFC's (Fig. 10).

3.2. Influence of opening ratio

The dimensions of the outlet port control the carbon dioxide exhaust from the flow channels of the anode. When a low opening ratio chamber is used, the performance of the cell decreases compared with using a high opening ratio. Low cell performance

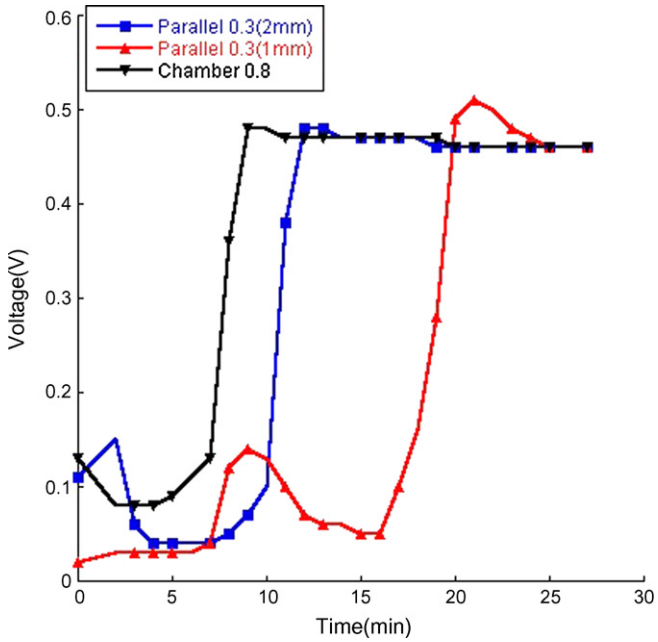

Fig. 8. Open-circuit voltage (OCV) and polarization curves in different channels: parallel channel (1 mm), parallel channel (2 mm), and chamber.

is obtained for channels with low opening ratios regardless of the channel shapes (Fig. 9). Therefore, the opening ratio is the key factor that affects the performance in these experiments. The peak performance is achieved when the chamber opening ratio is 0.8. The output power is 10.2 mW cm^{-2}. It is considered that the opening ratio affects the removal of product and by-product such as carbon dioxide and carbon monoxide in the anode. Carbon monoxide weakens catalyst activity and decrease the life-cycle of the catalyst [21–23]. It is concluded that a higher opening ratio leads to a more active electrochemical reaction between the reactants and the catalyst by proper venting of these products.

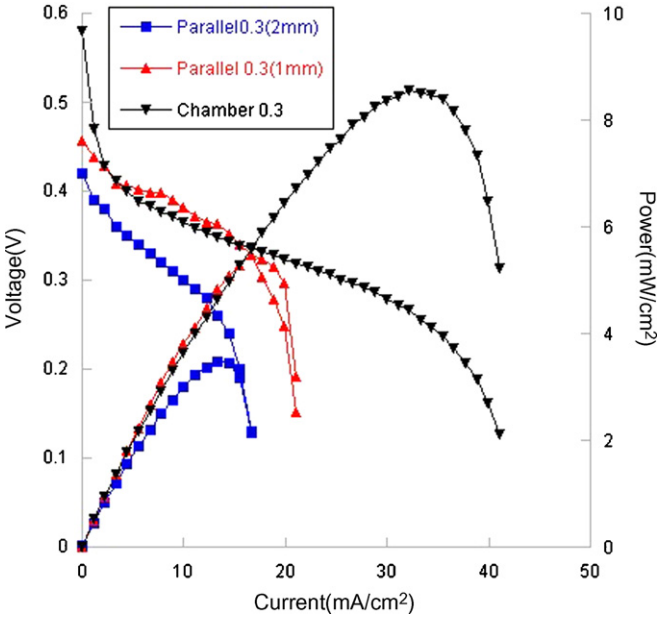

Fig. 9. Performance comparison of different flow channels in same opening ratio 0.3.

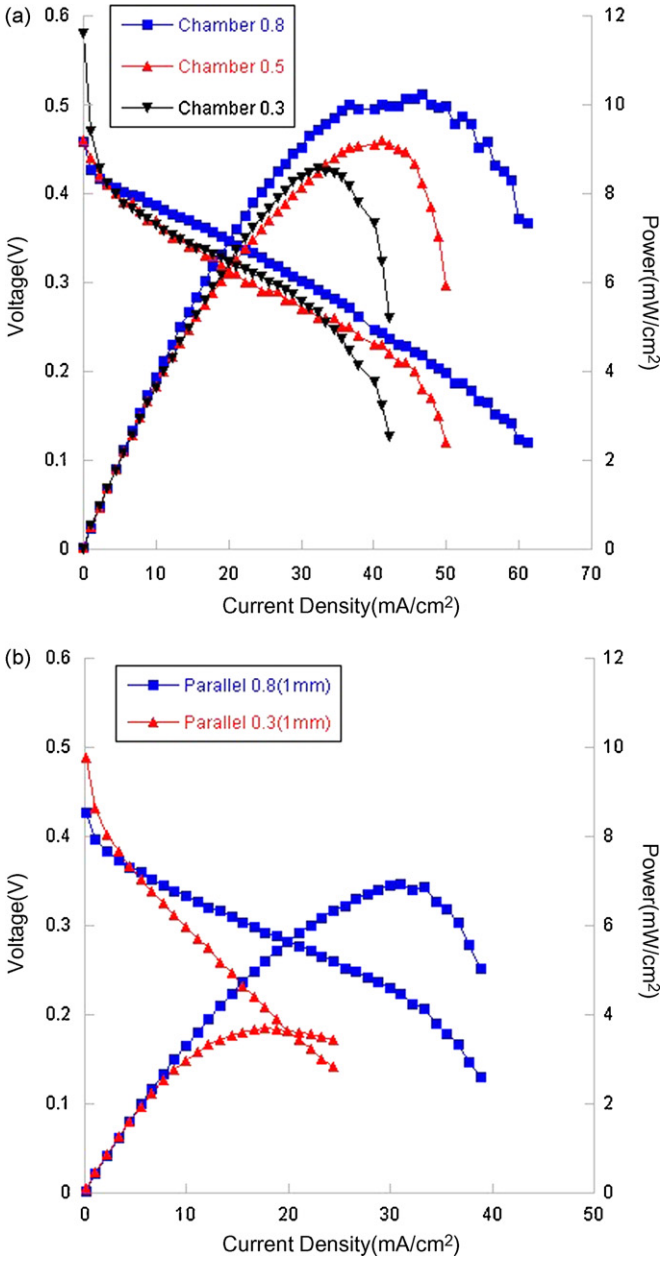

Fig. 10. Performance comparison of flow channels with different opening ratios: (a) different opening ratios in same chamber channel and (b) different opening ratios in same.

3.3. *Performance variation during 24 h operation*

The variation in the performance of passive DMFCs during 24 h is presented in Fig. 11. The cell was operated at 0.35 V, with a liquid methanol flow rate of 0.4 ml h^{-1} supplied by a syringe pump. The cell current was monitored without interruption during the test. On average, the performance of chamber type of opening ratio 0.8 is higher than any other type of flow channel. The performance of parallel channels is lower than that of a chamber type with an opening ratio 0.3. Parallel channels with low opening ratio have even lower performance. The chamber type (opening ratio 0.8) shows an abrupt performance drop at around 5 and 22 h. The performance drop of chamber type (opening ratio 0.8) is similar to the temperature drop. The performance of the cell with a low opening ratio (0.3) was poor during 24 h of operation for both parallel channel

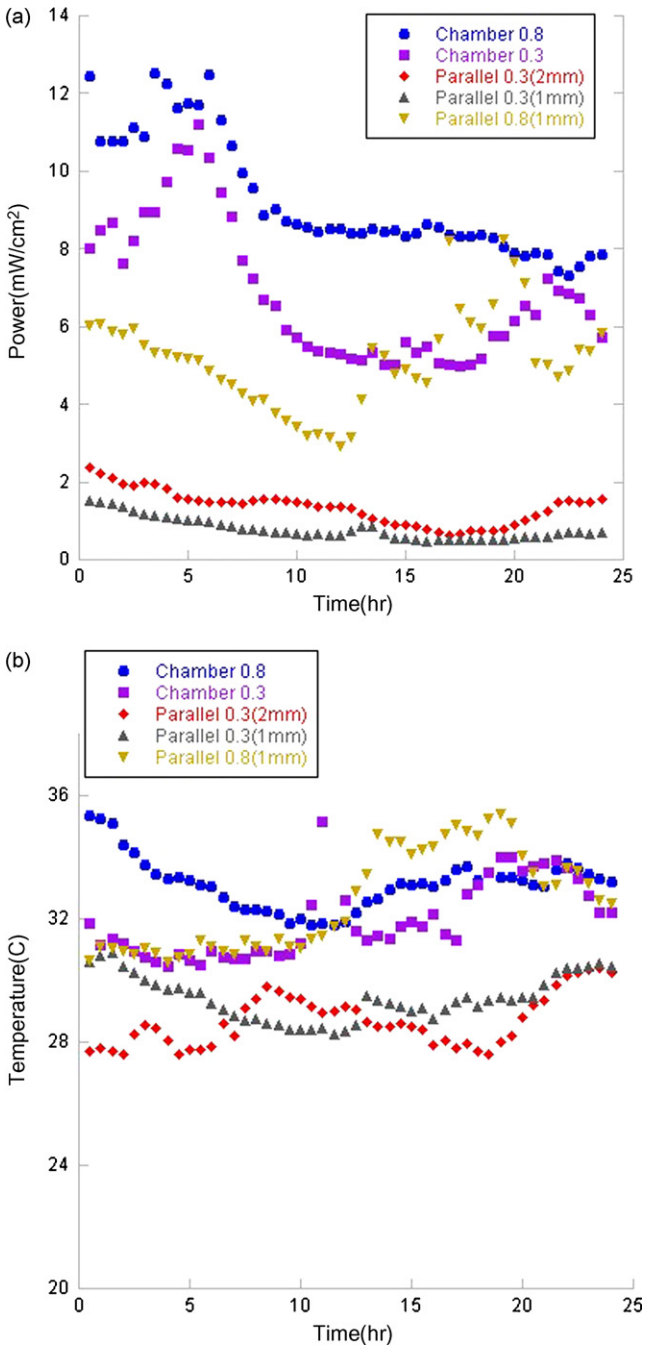

Fig. 11. Comparison of performance and temperature in different flow channels for 24 h: (a) performance variation and (b) temperature variation.

(1 mm) and parallel channel (2 mm) types. From the experimental data, the system of the chamber type has a fuel efficiency of 0.299%, based on 24 h of operation at 0.35 V with a methanol flow rate of 0.4 ml h^{-1}. The fuel efficiency is obtained from the equation:

$$\eta_{\mathrm{MeOH}} = \frac{\int_{t_o}^{t} P_{\mathrm{MeOH,\,rxn}}}{\int_{t_o}^{t} P_{\mathrm{MeOH,\,supplied}}} \tag{2}$$

where P is the power and t is the time. The denominator is the theoretical energy available from the supplied methanol during the operation, and the numerator is the total electrical work done by the fuel cell during the experiment. The Faradaic efficiency is:

$$\eta_{\mathrm{Faraday}} = \frac{\int_{t_o}^{t} I_{\mathrm{current,\,rxn}}}{\int_{t_o}^{t} I_{\mathrm{current,\,rxn}} + \int_{t_o}^{t} I_{\mathrm{current,\,crossover}}} \tag{3}$$

where I is the current and t is time. The denominator is sum of the amount of fuel used in current generation and the amount of fuel consumed by methanol crossover and other reactions during the operation. The numerator is the amount fuel used in current generation [24]. The Faraday efficiency of this system is 1.037% under the same conditions.

3.4. Temperature variation during 24 h of operation

The temperature variation of each flow channel is similar to the performance variation. The average temperature of the chamber type with an opening ratio 0.8 is higher than any other configuration. Also, abrupt temperature changes are observed for the chamber type with an opening ratio of 0.3 and a parallel channel (1 mm) with an opening ratio 0.8. The average temperature of chamber (opening ratio 0.3) is 32 °C. However, it increases abruptly to 36 °C after 11 h of operation. In Fig. 11, in spite of the abrupt temperature increase, the power density decreases slightly during the same time range. It is suspected that a change of methanol crossover rate may cause this phenomenon.

4. Conclusions

A passive air-breathing DMFC has been designed, fabricated and tested. The key parameters in the operation of the passive DMFC are flow channel types and opening ratios at the anode. Among the various flow channel configurations, chamber configurations are found to be the best for maximizing the performance. Consequently, the chamber type is more efficient than the parallel type for supplying methanol vapour. The higher the opening ratio, the higher is the performance in the experiments where the highest opening ratio is 0.8 for methanol vapour feeding. The power density of the chamber configuration with an opening ratio of 0.8 is 10.2 mW cm^{-2}. The opening ratio affects the differential pressure in the flow channels and the supply of methanol. A higher opening ratio helps the removal of product at the anode improves the performance. During 24 h of operation, the peak performance of the chamber configuration (opening ratio 0.8) is 12.2 mW cm^{-2}, and the average power density is around 9 mW cm^{-2} at ambient pressure and room temperature. In the same experiment, the trend of the temperature change of the cathode is similar to the variation in performance. An abrupt change of temperature is also observed, which is considered to be strongly related to a change in methanol crossover. The performance abruptly decreases due to methanol crossover at around 11 h (Fig. 11).

Acknowledgements

This work was sponsored by the Samsung Advanced Institute of Technology and the Brain Korea 21 program.

References

[1] M. Baldauf, W. Preidel, J. Power Sources 84 (1999) 161–166.
[2] S. Wasmus, A. Kuver, J. Electroanal. Chem. 461 (1999) 14–31.
[3] A. Heinzel, V.M. Barragan, J. Power Sources 84 (1999) 70–74.
[4] J. Cruickshank, K. Scott, J. Power Sources 70 (1998) 40–47.
[5] X. Ren, P. Zelenay, S. Thomas, J. Davey, S. Gottesfeld, J. Power Sources 86 (2000) 1111.
[6] D.H. Jung, C.H. Lee, C.S. Kim, D.R. Shin, J. Power Sources 71 (1998) 169–173.
[7] Y.H. Chan, T.S. Zhao, R. Chen, C. Xu, J. Power Sources 178 (2008) 118–124.

[8] Y.J. Kim, B. Bae, M. Aulice Scibioh, E.A. Cho, H.Y. Ha, J. Power Sources 157 (2006) 253–259.
[9] B. Bae, B.K. Kho, T.H. Lim, I.H. Oh, S.A. Hong, H.Y. Ha, J. Power Sources 158 (2006) 1256–1261.
[10] H.K. Kim, J. Power Sources 162 (2006) 1232–1235.
[11] L.S. Sarma, C.H. Chen, G.R. Wang, K.L. Hsueh, C.P. Huang, H.S. Sheu, D.G. Liu, J.F. Lee, B.J. Hwang, J. Power Sources 167 (2007) 358–365.
[12] M.K. Jeon, K.R. Lee, K.S. Oh, D.S. Hong, J.Y. Won, S. Li, S.I. Woo, J. Power Sources 158 (2006) 1344–1347.
[13] M. Inaba, M. Sugishita, J. Wada, K. Matsuzawa, H. Yamada, A. Tasaka, J. Power Sources 178 (2008) 699–705.
[14] J.J. Hwang, S.D. Wu, L.K. Lai, C.K. Chen, D.Y. Lai, J. Power Sources 161 (2006) 240–249.
[15] Y.H. Pan, J. Power Sources 161 (2006) 282–289.
[16] C.Y. Chen, P. Yang, J. Power Sources 123 (2003) 37–42.
[17] J.J. Martin, W. Qian, H. Wang, V. Neburchilov, J. Zhang, D.P. Wilkinson, Z. Chang, J. Power Sources 164 (2007) 287–292.
[18] H.Y. Cha, S.H. Kim, J.H. Jang, C. Miesse, J.H. Gil, H.R. Lee, A. Kundu, C.R. Jung, B. Ku, K.S. Chae, Y.S. Oh, Meet. Abstr. Electochem. Soc. 701 (2007) 187.
[19] Z. Qi, C. He, A. Kaufman, J. Power Sources 111 (2002) 239–247.
[20] W. Lee, H. Kim, T.K. Kim, H. Chang, J. Membr. Sci. 292 (2007) 29–34.
[21] T. Matsui, K. Fujiwara, T. Okanish, R. Kikuchi, T. Takeguchi, K. Eguchi, J. Power Sources 155 (2006) 152–156.
[22] A.A. Shah, P.C. Sui, G.-S. Kim, S. Ye, J. Power Sources 166 (2007) 198–204.
[23] H.S. Chu, C.P. Wang, W.C. Liao, W.M. Yan, J. Power Sources 159 (2006) 1071–1077.
[24] J.Y. Park, J.H. Lee, S.K. Kang, J.H. Sauk, I. Song, J. Power Sources 178 (2008) 181–187.